Tuning Charge Transfer Property of MoS_2 via Focused Laser Beam Based Technique

Kleon Ang Cunrong
Lim Yi Jing Carina
Rachel Pong Ruici
Dunman High School
10 Tanjong Rhu Road, Singapore 436895

Lili Gong
Sow Chorng Haur
Department of Physics
National University of Singapore
2 Science Drive 3, Singapore 117542

***Abstract*— Molybdenum disulfide (MoS_2), a transition metal dichalcogenide (TMDC), displays high potential in optoelectronics due to its strong absorption of visible light. Through the use of focused laser beams (FLB), the conductivity and photoresponsivity of MoS_2 can be tuned. FLB allows for precise and controlled modification of MoS_2, enabling fine tuning of charge transfer properties specifically for selected areas, essential for applications such as creating distinct p-doped and n-doped regions in p-n junctions for use in modern silicon chips. As-grown TMDCs reportedly contain a high density of chalcogen vacancies, reducing its electron mobility. We found that this can be countered by using FLB to atomically heal MoS_2, improving its conductivity and photoresponsivity. Au nanoparticles (NPs) sputtered on MoS_2 have been proven to demonstrate plasmonic enhancement of photocurrent of MoS_2 while improving its absorption of light. However, we found that while Au NPs decorated via FLB technique increases MoS_2's light absorption as predicted, it decreases its current and photoresponsivity. Past studies have also shown potential for increased conductivity and photoresponsivity of MoS_2 through amine-doping, prompting our investigation of the effect of urea, deposited via FLB technique, on MoS_2. The observed decrease in the dark current of MoS_2 after addition of urea disagrees with our hypothesis that n-doping occurs when urea was deposited on MoS_2. Additionally, effects of different metals used as electrodes on the conductivity of our samples were also investigated. Our results show that MoS_2 devices with Au/Cr electrodes sputtered on displayed greater ohmic behaviour than those with Al electrodes.**

I. BACKGROUND

Ultrathin sheets of transition metal dichalcogenides (TMDCs) have been demonstrated as layered semiconducting analogues of graphene [1] with sizeable band gaps [2], displaying unique electronic properties [3, 4] and atomically thin geometry [5]. Its 2-dimensional nature facilitates a high specific surface area, making it possible to employ surface and interface effects to improve the performance of electronic devices based on TMDCs [6].

Among these TMDCs, molybdenum disulfide (MoS_2) displays promising electrical [7-9] and optical [10, 11] properties with a significant band gap of 1.2eV for multi-layer MoS_2 [12, 13], as well as strong absorption of light in the visible band [14], resulting in its high potential in photocatalysis and photodetection [15, 16]. Practical applications of MoS_2 also include creating p-n junctions for use in modern silicon chips, which requires a clear separation of the p-doped and n-doped areas [17].

The advantage of using a focused laser beam is that it allows for structural manipulation of MoS_2. Besides having a high resolution and fast speed, high-power focused laser beams allow for precise and controlled thinning and patterning as well as property modification of MoS_2 in the nanoscale range. This enables fine tuning of charge transfer properties specifically for selected areas which is important for improving the functionality of MoS_2. Due to the increasing demand for monolayer TMDCs, laser-thinning methods have also been developed for the controlled layer-by-layer thinning of as-grown TMDCs post-synthesis to supplement the low production rates of exfoliation approaches [6]. Simultaneously, laser beams can be used as the control switches to operate devices manufactured with MoS_2.

As previous studies have shown that due to the compound nature and the higher volatility of chalcogenides, as-grown TMDCs contains a high density of chalcogen vacancies which reduces the electron mobility [18-21]. However, laser treatment has been shown to heal these defects in WSe_2 by filling the selenium vacancies with oxygen from the atmosphere, increasing the conductivity of WSe_2 [22]. We aim to investigate the effectiveness of this atomic healing via focused laser beam technique to improve the conductivity of MoS_2 films.

To further extend the potential of MoS_2, it is worthwhile to explore alternative modes of control over their photoelectric properties via chemical decoration of the MoS_2 films. Specifically, doping MoS_2 films with suitable noble metal nanoparticles is expected to provide an added channel for controlling the electrical properties of MoS_2 [23]. In particular, gold nanoparticles (Au NPs) are expected to increase the photoresponsivity and photocurrent of MoS_2 as Au NPs have demonstrated plasmonic enhancement of photocurrent of MoS_2 and the ability to improve its light absorption in previous works [3]. However, previous studies synthesised the Au NPs according to the Frens' method [24] or spin coating method [25], which does not allow precise control over the location of Au NPs deposited. With the recent development, it has been found that Au NPs can be selectively decorated onto MoS_2 films using a focused laser beam technique [26], allowing much higher control over the location of deposition of the Au NPs. We aim to test the effectiveness of this new focused laser beam technique of microlandscaping Au NPs to tune the charge transfer properties of MoS_2, specifically its photoresponsivity and photocurrent.

Additionally, past studies have pointed towards an improved photoresponsivity for aminopropyltriethoxysilane n-doped MoS_2 [27], which suggests potential for amine doped MoS_2 films. To further extend the focused laser beam technique to the surface deposition of amino compounds, we aim to investigate the effects of surface decoration of urea on ultrathin MoS_2 films via the focused laser beam technique on the charge transfer property of MoS_2.

II. Materials and Methods

A. Atomic Healing of MoS_2 via Focused Laser Beam Technique

Using a laser power of 10 mW, atomic healing will be conducted by moving the laser over the area between the electrodes in a raster pattern with 0.5 µm step length at a speed of 50 µm s^{-1}. The focused laser beam set-up is as shown in Figure 1.

B. Assembly of MoS_2 Samples into Devices

MoS_2 samples were assembled into devices for electrical testing as shown in Figure 2.

C. Modification of MoS_2 Samples via Drop Casting Method

Au NPs were locally deposited onto the surface of MoS_2 using a simple drop casting method. This method employs a focused laser beam technique (Figure 1). The device was placed onto a computer-controlled stage, and a 532 nm focused laser beam of 80 mW was used to create active nucleation sites in the selected area of the MoS_2 film between the metal (Al or Au/Cr) electrodes. Subsequently, $AuCl_3$ solution of concentration 1.0×10^{-4} mol dm^{-3} was dripped onto the substrate with activated nucleation sites. Au^{3+} in the solution becomes reduced by the active nucleation sites, resulting in the anchoring of Au NPs on these sites (Figure 3). The same procedure was repeated for the deposition of urea on another MoS_2 sample, using a urea solution of concentration 1.0×10^{-1} mol dm^{-3}.

D. Testing

Raman Spectroscopy, Scanning Electron Microscopy and Energy Dispersive Spectroscopy were carried out to characterise the samples. Electrical testing was then carried out to obtain Current-Voltage (I-V) and Current-Time (I-T) graphs. I-V testing was done with a starting voltage of -3V and ending voltage of 3V, with each measurement lasting 20s. I-T testing was done with a constant voltage of 3V, with each measurement lasting 30s. The laser shutter was opened at 10s and closed at 20s. The photoresponsivity of MoS_2 was then calculated using the following equation:

$$Photoresponsivity = \frac{I_{photo}-I_{dark}}{P_{effective}}, \text{ where}$$

$$P_{effective} = \frac{P_{laser}}{Area\ of\ laser\ spot} \times Area\ between\ electrodes$$

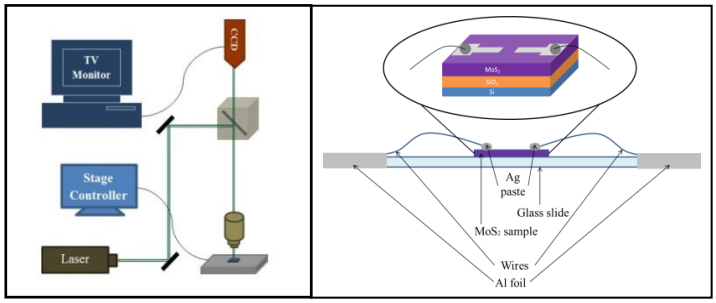

Figure 1 | Schematic diagram of focused laser beam set-up

Figure 2 | Side view of device

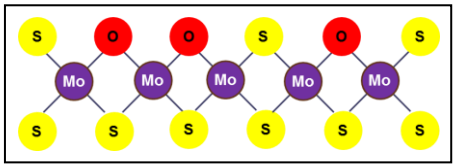

Figure 7 | Structure of MoS_2 after atomic healing by oxygen

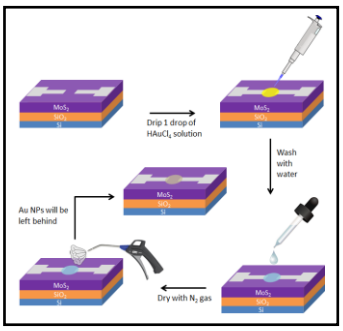

Figure 3 | Schematic diagram of deposition of Au NPs via drop casting method

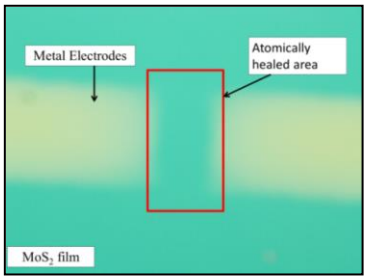

Figure 4 | Optical image of MoS_2 sample showing atomically healed area (in red box)

III. Results and Discussion

A. Testing Effect of Atomic Healing on MoS_2

1. Electrical Testing

A 10mW focused laser beam of 532 nm wavelength was used to atomically heal the MoS_2 sample. The laser was scanned over the area between the Al electrodes at a speed of 50 µm s^{-1} with a step size of 0.5 µm. After laser treatment, there is no observable difference in appearance between the atomically healed area and pristine MoS_2 when viewed with an optical microscope (Figure 4).

Firstly, a laser beam with varying powers (1 mW, 2 mW, 3 mW) was shone on the area between the electrodes and the resulting photocurrent was recorded. Our results show that 3 mW lasers induce the largest photocurrent on pristine MoS_2 as compared with the 1 mW and 2 mW lasers (Figure 5). However, the photoresponsivity for 2 mW laser was the highest for the pristine sample and that for 1 mW laser was the highest for the healed sample (Table 1). Hence, 2 mW laser, which balances between good photoresponsivity and photocurrent, was used to plot the graphs comparing different samples (Figure 6).

Comparing the pristine and atomically healed samples, the photoresponsivity of MoS_2 increased after laser treatment. This indicates that atomically healing the sample improves its conductivity. After laser treatment, the dark current increases from 52 nA to 85 nA and the laser-induced photocurrent increases from 17 nA to 25 nA (Figure 6). The increase in dark current suggests that the laser has effectively caused oxygen in the atmosphere to fill the sulfur vacancies in MoS_2 (Figure 7), preventing electrons from being trapped in these vacancies. After laser treatment, electrons in MoS_2 can flow at a faster rate, thus increasing dark current. Similarly, due to the increased conductivity after atomic healing, the photoresponsivity of the sample increased as well, as seen in the photoresponsivity calculations in Table 1.

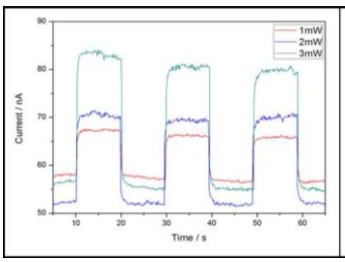

Figure 5 | I-T graph of pristine MoS_2 tested with 1mW, 2mW and 3mW laser

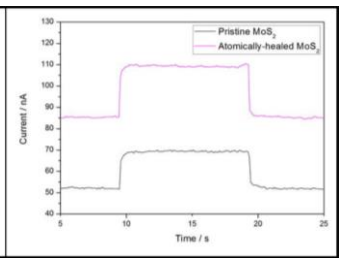

Figure 6 | I-T graph of pristine and healed MoS_2 at 2mW laser power

Table 1 | Photoresponsivity of MoS_2 sample before and after atomic healing

	Photoresponsivity (mA/W)	
Laser Power (mW)	**Pristine Sample**	**Atomically-Healed Sample**
1	0.73886	1.04981
2	0.76275	1.02697
3	0.73130	0.83199

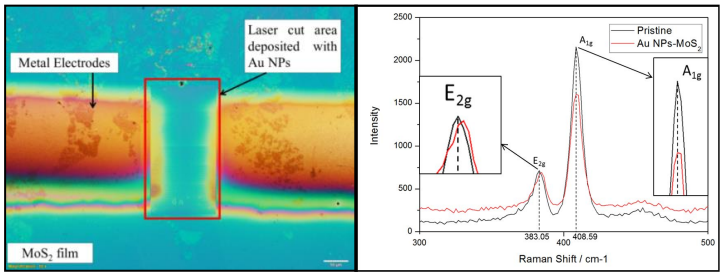

Figure 8 | Optical image of MoS_2 sample showing gold-MoS_2 area (in red box)

Figure 9 | Raman spectroscopy of pristine and gold-MoS_2 sample

B. Testing Laser-induced Photocurrent of Au NPs-decorated MoS_2

1. Characterisation

i. Raman Spectroscopy

In this section, Au NPs were deposited on a MoS_2 sample (Figure 8) using the drop casting method as mentioned above. Results from Raman Spectroscopy (Figure 9) on the pristine sample show the A_{1g} peak at 409 cm^{-1} and the E_{2g} peak at 383 cm^{-1}, which confirms that the sample is bulk-layer MoS_2 [28]. There is a decrease in layer number of MoS_2 after laser modification as seen from the decrease in the frequency difference of the of the A_{1g} and E_{2g} peaks from pristine MoS_2 to the modified MoS_2. The difference in Raman shift between the 2 Raman peaks decreased from 25.74 cm^{-1} in the pristine MoS_2 to 23.87 cm^{-1}, which shows a decrease from bulk layer to 4 layers [28]. Despite a decrease of the intensity of the A_{1g} and E_{2g} peaks due to the decrease in the relative amount of MoS_2, the increase in background intensity of the Raman graph suggests that the Au NPs were effective in enhancing the absorption of light by MoS_2.

ii. Scanning Electron Microscope (SEM)

It can be observed from the SEM images after Au NPs deposition that the laser modified area is brighter than the surrounding area, which suggests higher conductivity in the modified area (Figures 10 and 11). This confirms the presence and the controlled deposition of Au NPs in the laser modified area.

iii. Energy Dispersive Spectroscopy (EDS)

EDS on the gold-MoS_2 sample (Figure 12) shows that the ratio of the percentage by weight of Mo to that of Au is not very high, suggesting that there is a substantial amount of Au NPs deposited on the surface of MoS_2. The absence of Cl confirms that the remaining $AuCl_3$ solution has been thoroughly removed and that there are no Cl^- ions to conduct electricity on the surface of the gold-MoS_2.

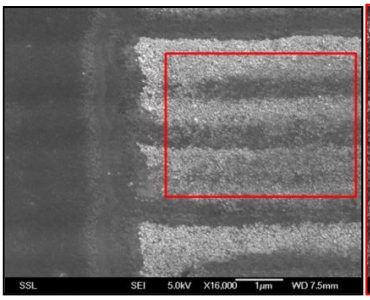

Figure 10 | SEM image of gold-MoS_2 sample at ×16,000 magnification with zoomed-in area (red box) shown in Figure 11

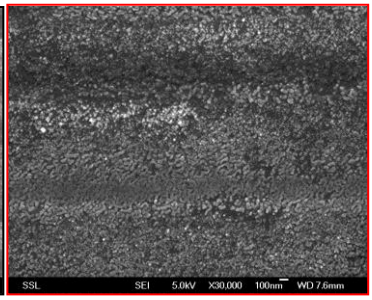

Figure 11 | SEM image of gold-MoS_2 sample at ×30,000 magnification

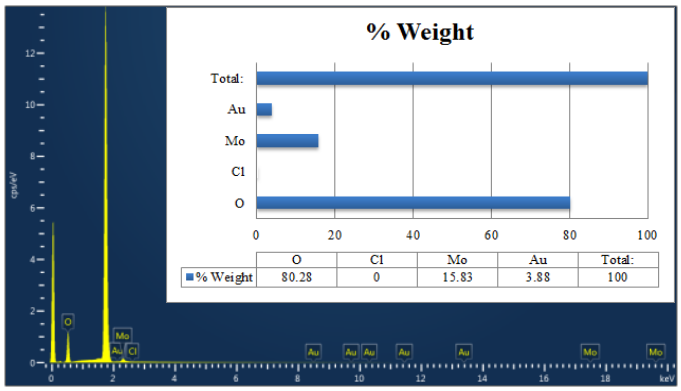

Figure 12 | EDS spectrum recorded on the gold-MoS_2 area showing percentage weight of selected elements

2. Electrical Testing

A laser beam of wavelength 532 nm was used to induce photocurrent as it was previously reported that Au NPs decorated MoS_2 possesses a photocurrent response peaked at the plasmon resonant wavelength of around 540 nm [14]. The sample was cut between the Al electrodes with the laser of 80 mW, and Au NPs were then deposited on the cut area via the drop casting method. Electrical testing was carried out after each stage and the I-T graph of the pristine, cut and gold-MoS_2 sample is shown below (Figure 13). The graph shows that after Au NPs were added, the dark current decreased from 49 nA to 46.5 nA and the laser-induced photocurrent decreased from 5 nA to 2 nA when Au NPs were added. The photoresponsivity also decreased when Au NPs were added for all laser powers (Table 2).

While it is expected that the photocurrent of MoS_2 should increase due to the enhanced absorption of light with Au NPs, with pristine MoS_2 naturally acting as an n-type semiconductor, the decrease in both the dark current and photocurrent after the deposition of Au NPs on MoS_2 suggests p-doping characteristics in gold-MoS_2. A proposed reason for this is that Au^{3+} ions from the $AuCl_3$ precursor, with an oxidation state of +3, are reduced to Au NPs, with an oxidation state of 0, indicating electron transfer from MoS_2 to Au^{3+} (Figure 14). Electrons are transferred from the laser-modified MoS_2 to the gold, reducing the density of charge carriers on MoS_2 and thus decreasing the dark current and photocurrent in the gold-MoS_2 sample. This theory can be verified by comparing electron concentrations before and after the deposition of Au NPs from Hall effect measurements in future experiments.

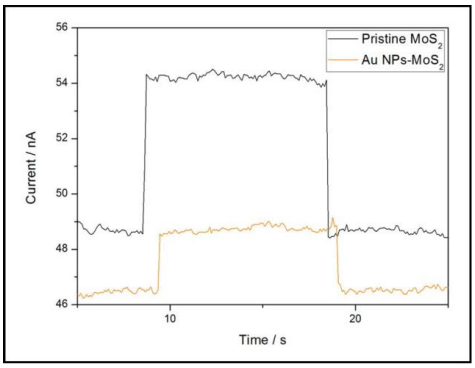

Figure 13 | I-T graph of pristine, cut, and gold-MoS_2 sample at 2mW laser power

Table 2 | Photoresponsivity of MoS_2 sample before and after laser cutting and after gold was added

	Photoresponsivity (mA/W)		
Laser Power (mW)	**Pristine Sample**	**Cut Sample**	**Au-MoS_2 Sample**
1	0.15856	0.12875	0.06081
2	0.12441	0.08899	0.04666
3	0.09372	0.07213	0.04064

C. Testing Laser-induced Photocurrent of Urea-decorated MoS_2

1. Characterisation

i. Raman Spectroscopy

From our results (Figure 15), the A_{1g} peak of Raman shift 408 cm^{-1} and E_{2g} peak of Raman shift 384 cm^{-1} shows that the sample is 4-layer MoS_2 [28]. The decrease in the intensity of both the A_{1g} and E_{2g} peaks shows that the relative amount of MoS_2 decreased after urea was added. The similar background intensity for pristine MoS_2 and urea-MoS_2 also suggests urea had no effect on the absorption of light.

ii. Energy Dispersive Spectroscopy (EDS)

EDS on the urea-MoS_2 sample (Figure 16) shows a relatively high percentage of C but low percentage of N. The high percentage of C, which arises from urea being an organic compound, confirms that urea was successfully deposited on the modified area, but the low percentage of N shows that the amide group of urea did not remain on the modified area.

2. Electrical Testing

Due to the nature of the batch of samples used as affected by the synthesis process, the photocurrent measured was very small, resulting in high percentage error and unreliability. Hence, electrical measurements for the photocurrent were omitted. As previously observed, the dark current decreased after laser cutting (Figure 17). However, it is worth considering urea deposition through alternative methods as we suspect that water may have influenced the electrical testing results, hindering the effectiveness of pinpointing the effect on the charge transfer properties solely due to the decoration of urea.

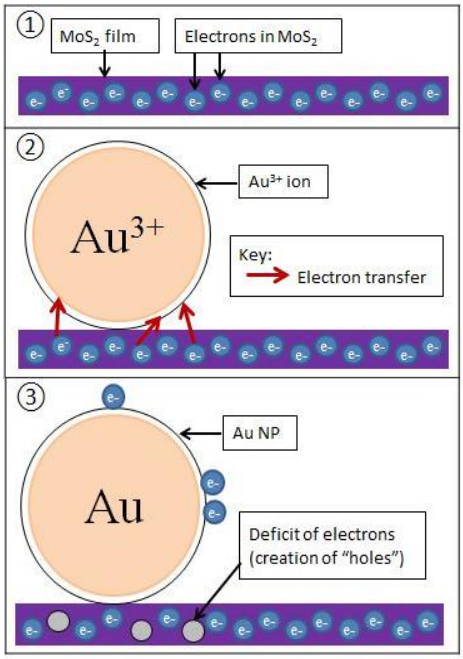

Figure 14 | Schematic diagram of the mechanism behind the deposition of Au NPs

① MoS_2 as n-type semiconductor with electrons as primary charge carriers.

② Introduction of Au^{3+} from $AuCl_3$ solution on MoS_2 surface. Electron transfer from MoS_2 to Au^{3+}.

③ Reduction of Au^{3+} to Au to form Au NPs. Electron transfer decreases the number of electrons in MoS_2, resulting in p-doped characteristics in MoS_2.

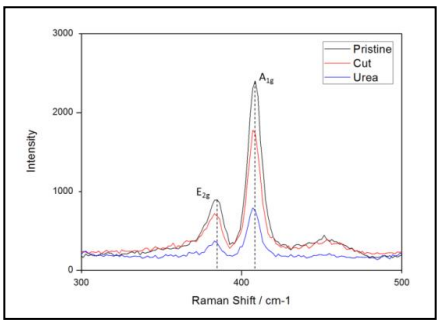

Figure 15 | Raman spectroscopy of pristine, cut and urea-MoS_2 sample

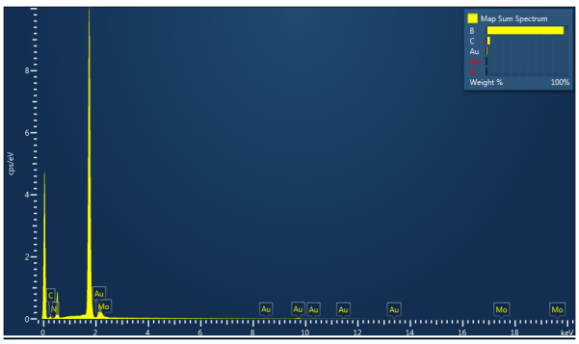

Figure 16 | EDS spectrum recorded on the urea-MoS_2 area

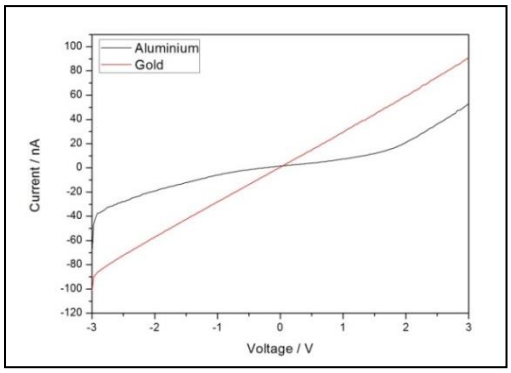

Figure 17 | I-V graph of pristine samples with Al and Au/Cr electrodes

D. Comparing Metals used as Electrodes

During the course of the experiment, we also investigated the effect of different metal electrodes on the charge transport behaviour of n-type MoS_2, with the metal electrodes being either Al or Au/Cr, with Cr (5 nm thickness) in contact with MoS_2 and Au (15 nm thickness) on top of Cr. The I-V curves obtained for voltages between -3 V and 3 V for samples with the Au/Cr electrodes were straighter, with greater ohmic behaviour as compared to the samples with Al electrodes (Figure 17), which we believe is due to the different Schottky barriers at the electrode-MoS_2 contact related to the work functions of the metal electrodes. Cr, with a higher work function of 4.5 eV, allowed a smaller Schottky barrier between the electrodes and MoS_2 and hence more ohmic behaviour than the Al electrodes of work function 4.28 eV. This suggests the possibility of exploring charge tuning of MoS_2 through using different metals in contact with MoS_2 film.

IV. CONCLUSION

In summary, we have successfully shown that atomic healing via the focused laser beam technique can be effectively extended to MoS_2 to increase its conductivity and photoconductivity. Au NPs decorated via focused laser beam, while has been effective in enhancing the absorption of light, does not increase the photoresponsivity of MoS_2. However, this method of decorating Au NPs has been shown to induce p-doped characteristics in MoS_2 instead. In addition, the decoration of urea on MoS_2 films has shown to be ineffective in the enhancing the conductivity through n-doping as previously hypothesized, but the use of other organic materials to tune the charge transfer properties of MoS_2 can be explored in future work. On top of that, our observations made of the various shaped of the I-V curves using different metal electrodes also suggests the possibility of tuning charge transfer properties of MoS_2 through investigating the effects of different metals on MoS_2 film.

V. ACKNOWLEDGEMENT

We would like to thank Lili Gong and Prof Sow Chorng Haur from the NUS Department of Physics for their guidance and continual support throughout the course of this project, as well as providing the facilities for conducting our research.

VI. REFERENCES

1. Rao, C.N.R. and A. Nag, *Inorganic Analogues of Graphene.* European Journal of Inorganic Chemistry, 2010. **2010**(27): p. 4244-4250.
2. Wilson, J.A. and A.D. Yoffe, *The transition metal dichalcogenides discussion and interpretation of the observed optical, electrical and structural properties.* Advances in Physics, 1969. **18**(73): p. 193-335.
3. Wang, Q.H., et al., *Electronics and optoelectronics of two-dimensional transition metal dichalcogenides.* Nat Nanotechnol, 2012. **7**(11): p. 699-712.
4. Chhowalla, M., et al., *The chemistry of two-dimensional layered transition metal dichalcogenide nanosheets.* Nat Chem, 2013. **5**(4): p. 263-75.
5. Novoselov, K.S., et al., *Two-dimensional atomic crystals.* Proceedings of the National Academy of Sciences of the United States of America, 2005. **102**(30): p. 10451-10453.
6. Lu, J., et al., *Interactions between lasers and two-dimensional transition metal dichalcogenides.* Chemical Society Reviews, 2016. **45**(9): p. 2494-2515.
7. RadisavljevicB, et al., *Single-layer MoS_2 transistors.* Nat Nano, 2011. **6**(3): p. 147-150.
8. Lembke, D. and A. Kis, *Breakdown of high-performance monolayer MoS_2 transistors.* ACS Nano, 2012. **6**(11): p. 10070-5.
9. Wang, H., et al., *Integrated circuits based on bilayer MoS_2 transistors.* Nano Lett, 2012. **12**(9): p. 4674-80.
10. Eda, G., et al., *Photoluminescence from Chemically Exfoliated MoS_2.* Nano Letters, 2011. **11**(12): p. 5111-5116.
11. Splendiani, A., et al., *Emerging Photoluminescence in Monolayer MoS_2.* Nano Letters, 2010. **10**(4): p. 1271-1275.
12. Mak, K.F., et al., *Atomically Thin MoS_2: A New Direct-Gap Semiconductor.* Physical Review Letters, 2010. **105**(13): p. 136805.
13. Fortin, E. and W.M. Sears, *Photovoltaic effect and optical absorption in MoS_2.* Journal of Physics and Chemistry of Solids, 1982. **43**(9): p. 881-884.
14. Lin, J., et al., *Plasmonic enhancement of photocurrent in MoS_2 field-effect-transistor.* Applied Physics Letters, 2013. **102**(20): p. 203109.
15. Yin, Z., et al., *Single-layer MoS_2 phototransistors.* ACS Nano, 2012. **6**(1): p. 74-80.
16. Lee, H.S., et al., *MoS_2 nanosheet phototransistors with thickness-modulated optical energy gap.* Nano Lett, 2012. **12**(7): p. 3695-700.
17. Li, H.-M., et al., *Ultimate thin vertical p–n junction composed of two-dimensional layered molybdenum disulfide.* Nature Communications, 2015. **6**: p. 6564.

18. Zhou, W., et al., *Intrinsic structural defects in monolayer molybdenum disulfide.* Nano Lett, 2013. **13**(6): p. 2615-22.

19. Yong, K.S., et al., *Calculation of the conductance of a finite atomic line of sulfur vacancies created on a molybdenum disulfide surface.* Physical Review B, 2008. **77**(20): p. 205429.

20. Caulfield, J.C. and A.J. Fisher, *Electronic structure and scanning tunnelling microscope images of missing-atom defects on MoS_2 and $MoTe_2$ surfaces.* Journal of Physics: Condensed Matter, 1997. **9**(18): p. 3671.

21. Komsa, H.-P., et al., *Two-Dimensional Transition Metal Dichalcogenides under Electron Irradiation: Defect Production and Doping.* Physical Review Letters, 2012. **109**(3): p. 035503.

22. Lu, J., et al., *Atomic Healing of Defects in Transition Metal Dichalcogenides.* Nano Letters, 2015. **15**(5): p. 3524-3532.

23. Shi, Y., et al., *Selective Decoration of Au Nanoparticles on Monolayer MoS_2 Single Crystals.* Scientific Reports, 2013. **3**: p. 1839.

24. Frens, G., *Controlled nucleation for the regulation of the particle size in monodisperse gold suspensions.* Nature Phys Sci, 1973. **241**: p. 20-22.

25. Lee, K.C.J., et al., *Plasmonic Gold Nanorods Coverage Influence on Enhancement of the Photoluminescence of Two-Dimensional MoS_2 Monolayer.* Scientific Reports, 2015. **5**: p. 16374.

26. Lu, J., et al., *Microlandscaping of Au Nanoparticles on Few-Layer MoS_2 Films for Chemical Sensing.* Small, 2015. **11**(15): p. 1792-1800.

27. Kang, D.-H., et al., *High-Performance Transition Metal Dichalcogenide Photodetectors Enhanced by Self-Assembled Monolayer Doping.* Advanced Functional Materials, 2015. **25**(27): p. 4219-4227.

28. Lee, C., et al., *Anomalous Lattice Vibrations of Single- and Few-Layer MoS_2.* ACS Nano, 2010. **4**(5): p. 2695-2700.